Cariogenic *Streptococcus mutans* produces strain-specific antibiotics that impair commensal colonization

Xiaoyu Tang[a,b]*, Yuta Kudo[b]*, Jonathon Baker[a], Sandra LaBonte[a,c], Peter A. Jordan[b], Shaun M. K. McKinnie[b], Jian Guo[d], Tao Huan[d], Bradley S. Moore[b,e] and Anna Edlund[a]

[a]Genomic Medicine Group, J. Craig Venter Institute, La Jolla, California, USA. [b]Scripps institution of oceanography, University of California, La Jolla, California, USA. [c]Department of Biochemistry and Biophysics, Texas A&M University and Texas AgriLife Research, College Station, Texas, USA. [d]Department of Chemistry, University of British Columbia, Vancouver, Canada. [e]Skaggs School of Pharmacy and Pharmaceutical Sciences, University of California, La Jolla, California, USA. *These authors contributed equally to this work.

Address correspondence to Bradley S. Moore, bsmoore@ucsd.edu or Anna Edlund aedlund@jcvi.org

***Streptococcus mutans* is a common constituent of dental plaque and an etiologic agent of dental caries (tooth decay). Here we elucidate a biosynthetic pathway, encoded by globally distributed strains of *S. mutans,* which produces a series of bioactive small molecules including reutericyclin and two *N*-acyl tetramic acid analogues active against oral commensal bacteria. This pathway may provide *S. mutans* with a competitive advantage, promoting dysbiosis and caries pathogenesis.**

The human microbiota consists of trillions of symbiotic microbial cells that not only help its host to digest dietary components(1-3), metabolize drugs(4-6), and regulate immune system(7-9) but also produce complex small molecules such as antimicrobial nonribosomal peptides (NRPs) and polyketides (PKs)(10-12). Recent computational mining efforts of genomes and metagenomes of the human microbiome revealed a vast diversity (~14,000) of putative biosynthetic gene clusters (BGCs) encoding small molecules across all human body sites(13), of which many represented NRP, PK and hybrid NRP-PK small molecules. A typical gut harbors 599 BGCs, while a typical oral cavity harbors 1061 BGC(13). Thus far, most research efforts have focused on characterization of BGCs and small molecules from the gut microbiome, leaving large knowledge gaps of crucial signaling molecules of the oral cavity.

The oral cavity harbors a high species diversity with over 700 bacterial species, which mainly colonize four physically distinct niches including dental plaque, tongue dorsum, buccal mucosa, and saliva(14). Residents of the dental plaque have been implicated in a variety of diseases, including dental caries, which affects more than a third of the world's population and results in approximately $300 billion in direct treatment costs to the global economy annually(15-17). Although caries is a polymicrobial disease caused by a dysbiosis in the dental plaque microbial community, *Streptococcus mutans*, with its copious acid production and prodigious biofilm formation, is still considered a primary etiologic agent(18, 19). To persist in the dental

51 plaque community and cause disease, *S. mutans* must be able to outcompete commensal
52 bacteria directly.

53 Small molecules produced by BGCs are increasingly recognized to play major roles in
54 species-species communication and interactions(10, 13), and a recent study predicted 355 strain-
55 specific BGCs across 169 *S. mutans* genomes(20). Although the production of mutactins (a group
56 of bacteriocins) has been recognized for contribution to the colonization and establishment of *S.*
57 *mutans* in the dental biofilm(21), the roles of other genetically encoded small molecules in *S.*
58 *mutans* is barely explored, with exception of the mutanobactins. Mutanobactins are compounds
59 of hybrid polyketide synthase and nonribosomal peptide synthetase (PKS/NRPS) origin that
60 inhibit the morphological transition of *Candida albicans*(22). Previous bioinformatics efforts
61 identified an orphan hybrid PKS/NRPS BGC (recently designated *muc*)(20, 23), that is distributed
62 among a subset of *S. mutans* strains. Within *muc*, five biosynthetic proteins are highly
63 homologous (48%-69%) to cognates involved in the biosynthesis of reutericyclin (RTC)(24)
64 (**Supplementary Fig. 1** and **Fig. 1a**). RTC, which originated from the sourdough isolates of
65 *Lactobacillus reuteri*, acts as a proton ionophore antibiotic that modulates the microbial
66 community of sourdough(25, 26). Interestingly, we found that *S. mutans* strains encoding *muc*
67 were dispersed geographically and frequently associated with severe dental caries
68 (**Supplementary Table 1**). The goal of this study was to determine whether *muc* produces RTC
69 or RTC-like molecules, and if these molecules can affect inter-species competition in the oral
70 cavity.

71 To determine the product of *muc*, we utilized homologous recombination to delete the
72 gene *mucD*, which encodes an assembly line NRPS tridomain protein (**Fig. 1a**). We conducted
73 all our biosynthetic experiments in *S. mutans* B04Sm5, a strain bearing *muc*, which was isolated
74 from a child with severe early childhood caries(27). The wild type (WT) strain and Δ*mucD* mutant
75 were cultured and extracted for HPLC analyses. The results showed that the WT strain produced
76 four metabolites not present in the Δ*mucD* mutant (**Fig. 1b**). These molecules were purified via

77 preparative HPLC (**Supplementary Note 1**) and characterized by High-Resolution Mass
78 Spectrometry (HR-MS/MS), chemical synthesis, and/or one- and two-dimensional Nuclear
79 Magnetic Resonance (NMR) experiments to yield a group of tetramic acids, including RTC
80 (renamed RTC A, **1**), two new RTC analogues (RTC B (**2**) and RTC C (**3**)), and a new organic
81 acid (**4**) (**Fig. 1c**, **Supplementary Note 1**, **Supplementary Tables 2-3**, **Supplementary Figs. 2-**
82 **22**). During preparation of this manuscript, Chen and colleagues published the identification of **4**
83 (designated mutanocyclin (MUC)) using a new heterologous genetic system(23); however,
84 production of **1**-**3** in both heterologous host and wild type producers was not reported.

85 *Muc* is a ~13 kb hybrid NRPS-PKS pathway encoding nine proteins (**Supplementary**
86 **Table 5**). *In silico* analysis revealed that *mucD* to *mucE* encode the core assembly line protein
87 machinery (**Fig. 1a** and **Fig. 2a**). While MucD is a C-A-T tridomain protein, with specificity for
88 adenylating leucine, MucE contains an KS-T-TE module, as commonly present in the termination
89 modules of PKS assembly lines. Based on the enzymatic logic of thiotemplate-mediated assembly
90 line biosynthesis, we propose that **1**-**3** are assembled, respectively, from *trans*-2-decenoyl-ACP,
91 decenoyl-ACP, and *trans*-2-dodecenoyl-ACP starter units through elongation with leucine,
92 followed by elongation with a malonyl-CoA extender unit (**Fig. 2a**). Inspection of structures of **1**-**3**
93 suggested that the A domain of MucD appears to install a *D*-leucine residue into the final product.
94 To explore this hypothesis, we fed both [$^{13}C_1$] *L*- and *D*-leucine to cultures of *S. mutans* B04Sm5.
95 MS analyses of the purified **1** and **3** only revealed the incorporation of [$^{13}C_1$] *L*-leucine
96 (**Supplementary Figs. 23-24**). The same result was observed by feeding the original RTC
97 producer *L. reuteri* with the same isomers (**Supplementary Fig. 25**). These results indicate that
98 an unrecognized epimerization reaction is involved in **1**-**3** biosynthesis; however, no standard
99 epimerization (E) domain or dual functioning C/E domains could be found either in the assembly
100 line or encoded elsewhere in the BGC. Additionally, although a dual-function TE/E domain has
101 been characterized from the nocardicin (NOC) biosynthetic assembly line(28), MucTE shows very
102 low homology (20%/35%, identity/similarity) to the dual functioning NocTE domain.

103 The first three genes (*mucA-C*) encode a hydroxymethylglutaryl-CoA synthase (MucA), a
104 thiolase (MucB), and a hypothetical protein (MucC) (**Supplementary Table 5**), which show
105 homology to the three submits (PhlA, PhlB and PhlC, respectively) of a multicomponent C-
106 acetyltransferase involved in the acetylation of the type III PKS product phloroglucinol from
107 *Pseudomonas fluorescens* Q2-87(29, 30). As the combination of the three genes was also
108 identified in *rtc* (*rtcA*, *rtcC* and *rtcB*) from *L. reuteri* (24), the function of MucA–C is consistent with
109 introducing the acetyl group to the pyrrolidine ring of **1**-**3** (**Fig. 2a**). We additionally annotated four
110 genes downstream of the *mucA-E* operon encoding a small HXXEE domain-containing
111 membrane-protein (MucF) of unknown function, two TetR/AcrR family transcriptional regulators
112 (MucG and MucH), and one multidrug efflux pump (MucI) (**Supplementary Table 5**). Presumably,
113 they are not involved in the direct synthesis of **1**-**3**. To verify this hypothesis, we cloned the operon
114 from *mucA* to *mucE* into the pACYCDuet-1 vector to generate the plasmid pEXT06, in which the
115 operon is exclusively under control of a T_7 promoter. As expected, expression of *mucA-E* in
116 *Escherichia coli* BAP1 strain resulted in the production of at least four products, including **1**-**3** and
117 new compound **5** (**Fig. 2b** and **Supplementary Fig. 26**). **5** was purified via preparative HPLC and
118 its structure was further confirmed as a new RTC analogue (RTC D) possessing a saturated C-
119 12 fatty acid side chain by MS and NMR analyses (**Supplementary Table 4**, **Supplementary**
120 **Fig. 26** and **Supplementary Figs. 27-30**). This result indicates that the first six genes *mucA-E*
121 indeed compose the minimal BGC for **1**–**3** production (**Fig. 2a**).

122 As the structure of **4** is consistent with the RTC core lacking the fatty acyl chain, we first
123 set out to detect whether the free fatty acid, *trans*-2-decenoic acid per compound **1**, is present in
124 the extract of *S. mutans* B04Sm5. HPLC analyses confirmed that *S. mutans* B04Sm5 readily
125 produced *trans*-2-decenoic acid (**Supplementary Fig. 31**). In contrast, it was not detected in the
126 pathway-deficient mutant *S. mutans* B04Sm5/Δ*mucD*. These findings suggested that **4** may be
127 derived from **1**-**3** via deacylation by an unknown enzyme. Interestingly, *trans*-2-decenoic acid is
128 a known *Streptococcus* diffusible signal factor (SDSF) isolated from many *Streptococcus*

129 species(31), which inhibits the hyphal formation of the opportunistic fungus *Candida albicans*.
130 Among the annotated pathway enzymes, only the function of MucF was unassigned. The MucF
131 protein sequence was subjected to a secondary structure prediction-based homology search
132 (Phyre2), which suggested it is a polytopic (five) transmembrane α-helical protein
133 (**Supplementary Fig. 32**) with low similarity (15%) to a viral protein (PDB 3LD1) with putative
134 hydrolase activity. To explore whether MucF might be involved in the deacylation of **1**-**3**, we
135 generated a *mucF* deletion mutant in *S. mutans* B04Sm5. HPLC analysis of the extract of mutant
136 cultures showed that the Δ*mucF* mutant not only increased the production of **1**-**3** by ~3-5 fold, but
137 also lost the ability to produce **4** (**Fig. 1b**). These findings strongly suggested that MucF is
138 essential for converting **1**-**3** to **4**. To further evaluate the function of MucF, we cloned and
139 expressed *mucF* in *E. coli* and incubated **1** with the *E. coli*/*mucF* cell lysate, leading to the *in vitro*
140 production of the deacylated **4** (**Fig. 2c**). In contrast, no conversation was detected in the control
141 experiment (*E. coli* carrying empty vector) (**Fig. 2c**). To further support this observation, we
142 inserted a copy of *mucF* into the secondary expression site of pEXT06, resulting in the plasmid
143 pEXT07. Its expression in *E. coli* BAP1 further led to the formation of **4** (**Fig. 2b**). Collectively,
144 these mutations, *in vitro*, and *in vivo* expression studies support the hypothesis that MucF is a
145 newly recognized deacylase responsible for converting **1**-**3** to **4**. Notably, MucF showed sequence
146 similarity to a large group of hypothetical proteins from the genomes of bacteria associated with
147 the human gut and skin (**Supplementary Fig. 33**). We therefore speculate MucF joins a large
148 family of unrecognized deacylases that may play important roles within the human microbiota.
149 Next, we took two approaches to determine whether RTCs and MUC play roles in
150 mediating inter-species bacterial competition. Frist, we used a plate-based competition assay, in
151 which a colony of *S. mutans* UA159 (a model organism for caries disease), *S. mutans* B04Sm5
152 (producing **1**-**4**), *S. mutans* B04Sm5/Δ*mucD* (**1**-**4** deficient strain), or *S. mutans* B04Sm5/Δ*mucF*
153 (producing **1**-**3** exclusively) was plated next to nascent colonies of other oral bacteria, including
154 *Rothia mucilaginosa*, *S. sanguinis*, *S. gordonii*, *S. mitis*, *S. pneumoniae*, and *S. salivarius* (**Fig.**

155 **3**). In general, *S. mutans* B04Sm5 exhibited greater inhibition of neighbors than the *S. mutans*
156 model strain UA159. In contrast, *S. mutans* B04Sm5/Δ*mucD*, which lacks the production of
157 compounds **1**-**4**, dramatically exhibited reduced inhibition of its neighbors. For instance, *S. mutans*
158 B04Sm5 impaired the growth of *S. sanguinis* completely, while *S. mutans* B04Sm5/Δ*mucD* only
159 showed slight inhibition of *S. sanguinis*. Furthermore, although the growth of *S. mutans*
160 B04Sm5/Δ*muc*F was impaired by overproducing **1**-**3**, it exhibited the strongest inhibition of
161 neighbors among all tested strains. *S. sanguinis* is one of the predominant species of the
162 indigenous oral biota colonizing dental plaque, which is normally associated with healthy dental
163 biofilm(32). The antagonistic relationship between *S. sanguinis* and *S. mutans* is well-
164 characterized, and plays an important role in caries development(33, 34). Therefore, we
165 determined the Minimum Inhibitory Concentration (MIC) of isolated **1** and **4** against the *S.*
166 *sanguinis* ATCC 49296. Remarkably, we observed significant antibacterial activity of **1** against
167 the *S. sanguinis* (MIC=3.1 μM), However, **4** did not show any antibacterial activities against *S.*
168 *sanguinis* up to a concentration of 2 mM. These results provide compelling support that the *muc*
169 pathway, through compounds **1-3,** provides a competitive advantage for *S. mutans* B04Sm5 by
170 inhibiting the growth of its competitors. The increased competitive fitness conferred by *muc* is
171 likely to increase the virulence *S. mutans* strains bearing the gene cluster. As *S. mutans* is an
172 exceptionally productive biofilm-former, higher numbers of *S. mutans* are likely to increase plaque
173 biofilm formation and promote the dysbiosis which leads to the formation of caries lesions.
174 Interestingly, Chen and colleagues showed that **4** can significantly suppress the infiltration of
175 leukocytes ($CD45^+$ cells) into the Matrigel plug in a mice model, suggesting an anti-inflammatory
176 activity(23).

177 In summary, we describe a versatile biosynthetic pathway from an oral pathogen *S.*
178 *mutans* B04Sm5, which can produce three types of compounds with divergent biological activities.
179 These include three *N*-acyl tetramic acids (**1**-**3**) that display antibacterial properties against oral
180 commensal bacteria, a new organic acid (**4**) with a reported anti-inflammatory activity in a mice

181 model(23), and a previously characterized SDSF with the ability to interact with pathogenic oral
182 fungi(31). Although two antibiotics have been discovered from the commensal bacteria of human,
183 including lactocillin(13) and lugdunin(35), RTCs, to our knowledge, are the first group of low
184 molecular weight antibacterial molecules identified from a human opportunistic pathogen. While
185 this study merely scrapes the "tip of the iceberg" of the recently identified oral biosynthetic
186 potential(13, 36), these findings clearly exemplify that deeper exploration of leads provided by
187 genome mining studies will help elucidate the complex ecological underpinnings of the human
188 microbiome and its relationship to disease.
189

190 # METHODS

191 **General methods**. A complete list of the primers, plasmids, and strains used in this study can be
192 found in **Supplementary Table 6**. PCR products were amplified with PrimeSTAR HS DNA
193 polymerase (Clontech Laboratories, Inc., USA). DNA isolations and manipulations were carried
194 out using standard protocols. *Escherichia coli* strains were cultivated in LB medium (Thermo
195 Fisher Scientific, USA) supplemented with appropriate antibiotics. *S. mutans* B04Sm5 and its
196 respective derivatives were all grown on Brain Heart Infusion (BHI) agar or liquid medium (BD
197 Biosciences, USA) at 37 °C in a CO_2 incubator (5% CO_2/95% air). *Lactobacillus reuteri* LTH2584
198 was also grown on MRS medium (BD Biosciences, USA) or agar at 37 °C in a CO_2 incubator (5%
199 CO_2).
200

201 **Production, extraction, and detection of reutericyclins (1-3) and mutanocyclin (4) from *S.***
202 ***mutans***. 50 milliliters of BHI medium were inoculated with a loop of glycerol stock of *S. mutans*
203 or a mutant thereof overnight. Thirty milliliters of preculture was inoculated into 3 liters of BHI
204 medium containing 1% glucose. After 12 hours incubation, 60 g of autoclaved Amberlite XAD7-
205 HP resin (Sigma-Aldrich, USA) was added to the cultures. The cultures were incubated for

206 another 36 hours at 37 °C in a CO_2 incubator (5% CO_2). The resin was recovered and washed
207 twice with water (200 mL) and the extract was subsequently extracted twice with ethyl acetate
208 (400 mL in total). The organic phase was evaporated, and extracts were dissolved in 2 mL
209 methanol. Each extract was monitored at 280 nm during separation by HPLC using a Kinetex®
210 C18 100 Å, LC Column (5 μm, 150 × 2.1 mm; Phenomenex, US) as follows: 0-15 min, 30% B;
211 15-16 min, 30%-100% B; 16-25 min, 100% B; 26-27 min, 100%-30% B; 28-35 min, 30% B (solvent
212 A: H_2O/TFA (999:1, v/v); solvent B: CH_3CN/TFA (999:1)).
213
214 **Construction of *S. mutans* knockout plasmids.** A 1010-bp fragment containing the
215 spectinomycin resistance gene (*spec*^{R}) was amplified from pCAPB2(37) with primers spec_fwd
216 and spec_rev (**Supplementary Table 6**). The left (532 bp) and right (555 bp) flanks of *mucD* were
217 amplified from the genomic DNA of *S. mutans* B04Sm5 with the primer pairs of mucD_KO_L-
218 fwd/mucD_ KO_L-rev and mucD_ KO_R-fwd/mucD_ KO_R-rev (**Supplementary Table 6**),
219 respectively. These three PCR products were assembled with a double digested pUC19 (PstI and
220 EcoRI) using a NEBuilder HiFi DNA Assembly kit (New England Biolabs, USA), which resulted in
221 the vector pEXT01. Amplification of the left (602 bp) and right (611 bp) homology arms for
222 knocking out *mucF* were accomplished with primer pairs mucF_ KO_L-fwd/mucF_ KO_L-rev and
223 mucF_ KO_R-fwd/mucF_ KO_R-rev (**Supplementary Table 6**), respectively. These two PCR
224 products and *spec*^{R} cassette were further cloned into pUC19 to give pEXT02 using the method
225 described above. Vector clones were verified by restriction analysis and sequencing.
226
227 **Generation of Δ*mucD* and Δ*mucF* mutants.** The disruption cassettes were amplified from
228 pEXT01 (2159 bp) and pEXT02 (2159 bp) using primer pairs mucD_KO_L-fwd/mucD_ KO_R-rev
229 and mucF_ KO_L-fwd/mucF_ KO_R-rev (**Supplementary Table 6**), respectively. PCR products
230 were digested by DpnI and then purified using the QIAquick PCR Purification Kit (Qiagen, USA).
231 The disruption cassettes were transferred to *S. mutans* B04Sm5 by a previously reported

232 protocol(38). Spectinomycin resistance clones were selected by growth on BHI agar
233 supplemented with 500 μg/mL spectinomycin, confirmed by PCR and sequencing, and
234 designated as *S. mutans* B04Sm5/Δ*mucD* and *S. mutans* B04Sm5/Δ*mucF*.
235
236 **Generation of *muc* expression plasmid.** The 8.6-kb DNA region containing *mucA-E* was PCR
237 amplified from the genomic DNA of *S. mutans* B04Sm5 in two fragments (each approximately 4
238 kb) with primer pairs mucA-E_ fwd1/ mucA-E_rev1 and mucA-E_fwd2/ mucA-E_rev2
239 (**Supplementary Table 6**). These fragments were cloned into the XhoI site of pACYCDuet-1 by
240 a NEBuilder HiFi DNA Assembly kit (New England Biolabs, USA), resulting in the plasmid pEXT06.
241 To construct pEXT07, *mucF* was amplified with primers mucF-coexp_fwd and mucF_coexp_rev.
242 PCR product and pEXT06 were digested with the restriction enzyme pair NcoI/BamHI and ligated
243 with T4 DNA ligase (New England Biolabs, USA). The resulting vectors were verified by restriction
244 analysis and sequencing. pEXT06 and pEXT07 were transformed into *E. coli* BAP1, respectively.
245
246 **Expression, extraction, and detection of *muc* expression in *E. coli* BAP1.** *E. coli* BAP1(39)
247 containing pEXT06 or pEXT07 were cultivated on LB plates supplemented with 1% glucose and
248 50 μg/mL chloramphenicol at 37 °C. The following day, a loop of *E. coli* cells was transferred for
249 precultures grown at 37 °C in 10 mL LB medium supplemented with 1% glucose and 50 μg/mL
250 chloramphenicol for 4-5 h. One microliter of each preculture was transferred to 50 mL of fresh LB
251 with the same supplements and grown at 37 °C to an OD_{600} of 0.4 to 0.6. Cultures were induced
252 with 200 μM IPTG and incubated for an additional 12-14 h at 30°C with shaking (220 rpm).
253 Cultures were harvested and 1 mL of H_2O supplemented with 0.5 mg/mL lysozyme was added to
254 the pellets. Cells were disrupted by sonication at room temperature. The lysates were acidified
255 with acetic acid (1% final concertation) and extracted by twice with an equal volume of EtOAc.
256 The organic phase was evaporated, resuspended in MeOH (0.2 mL), and filtered through
257 Acrodisc MS PTFE Syringe filters (Pall Inc., Ann Arbor, MI, USA) prior to HPLC analysis. Each

258 extract was monitored at 280 nm during separation by HPLC using a Kinetex® C18 100 Å, LC
259 Column (5 µm, 150 × 2.1 mm; Phenomenex, US) as follows: 0-10 min, 30% B; 10-11 min, 30%-
260 100% B; 11-25 min, 100% B; 26-27 min, 100%-30% B; 28-35 min, 30% B (solvent A: H_2O/TFA
261 (999:1, v/v); solvent B: CH_3CN/TFA (999:1)).

262 **Feeding experiments for biosynthetic pathway study**. *S. mutans* B04Sm5 was cultivated in
263 50 mL BHI medium supplemented with 1% glucose and 200 mg/L isotope-labeled [$^{13}C_1$] *L*- or *D*-
264 leucine (Sigma-Aldrich, USA). The compounds were extracted and isolated using the method
265 described above. Each extract prepared was dissolved in 100 µL MeOH for MS analysis using
266 the method described in the supplementary information (**Supplementary Note 1**).

267

268 **Expression and activity mensuration of MucF in *E. coli*.** Primer pair mucF_pET_fwd/mucF_
269 pET_rev (**Supplementary Table 6**) was used for amplification of *mucF* from the genomic DNA of
270 *S. mutans* B04Sm5. The PCR product was cloned into the NcoI and XhoI sites of pET28a to
271 obtain pEXT26 (with a C-terminal His-tag). Next, pET28a and pEXT26 were transferred into *E.*
272 *coli* Rosetta2^{TM} (DE3)pLys, respectively. Single clones were picked for precultures grown
273 overnight at 37°C in TB broth (Thermo Fisher Scientific, USA) with 50 µg/mL kanamycin and
274 50µg/mL chloramphenicol at 37°C. One microliter of preculture was transferred to 1 L of fresh TB
275 broth with the same antibiotics and grown at 37°C to an OD600 of 0.4 to 0.6. Cultures were
276 induced with 500 µM IPTG and incubated for an additional 16 h at 18°C with shaking (220 rpm).
277 Cultures were harvested and 10 mL of buffer (50 mM Tris-HCl, pH 8, 150 mM NaCl, 10% glycerol)
278 supplemented with 0.5 mg/mL lysozyme and 0.5 mM PMSF was added to the pellets. Cells were
279 disrupted by sonication at 4°C. The lysate was used for MucF activity testing. The assay mixture
280 for the reaction (100 µL) consisted of 96 µL *E. coli* lysate (both carrying empty pET28a or pEXT26)
281 and 4 µl reutericyclin A (**1**) solution (6.6 mM, 80% EtOH). The reaction solutions were prepared
282 on ice and incubated at 37°C for 10 min, 30 min and 60 min. Reactions were terminated by the
283 addition of 1 µL acetic acid and then extracted twice with 200 µL EtOAc. After centrifugation of

284 the assay at 12,000 *g* for 10 min, the organic phase was evaporated and resuspended in 100 µL
285 MeOH (0.2 mL). The extracts were monitored by HPLC.
286
287 **Agar plate-based assays.** The interspecies competition assays with *S. mutans* (UA159,
288 B04Sm5, Δ*mucD,* Δ*mucF*), *R. mucilaginosa, S. gordonii*, and *S. sanguinis, S. mitis, S.*
289 *pneumoniae,* and *S. salivarius* were performed as described previously(40), with some
290 modifications. 8 µl of overnight cultures of *S. mutans* strains were inoculated onto BHI agar and
291 incubated at 37°C under a 5% CO_2/95% air atmosphere (vol/vol). After a 24 h incubation period,
292 an overnight culture of the indicated competing species was inoculated next to the *S. mutans* and
293 the plates were incubated for an additional 24 h and subsequently photographed.
294

295 ## Acknowledgments

296 The authors thank Y. Li (NYU College of Dentistry, USA) for providing *S. mutans* strain B04Sm5,
297 M.G. Gänzle (University of Alberta, Canada) for providing *L. reuteri* LTH2584 strain, C. Khosla
298 (Stanford University, USA) for *E. coli* BAP1, and J.J. Zhang (Massachusetts Institute of
299 Technology, USA), M.S. Donia (Princeton University, USA) and M.A. Fischbach (Stanford
300 University, USA) for valuable discussions. This work was supported by NIH grants R00-
301 DE0245543 and R21-DE028609-01 to A.E., R01-GM085770 to B.S.M., and F32-DE026947 to
302 J.B., and the Japan Society for Promotion of Science Overseas Research Fellowship to Y.K.
303

304 ## Author contributions

305 X.T. and A.E. designed the research and X.T. analyzed the *muc* pathway. X.T. generated and
306 analyzed the mutants, performed the biochemical experiments and the heterologous expression
307 experiments. Y. K. and X.T. purified the compounds and elucidated the structures of all
308 compounds. X.T., P.A.J. and S.M.K.M. performed the chemical synthesis. X.T., Y.K., J.G. and

309 T.H. performed mass spectrometry experiments and analyzed mass spectrometry data. X.T., J.B.
310 and S.L. designed and performed the agar plate-based assays. X.T., Y.K., J.B., A.E. and B.S.M.
311 wrote the manuscript. All authors analyzed and discussed the data and contributed to the writing
312 of the manuscript.
313

314 ## Competing financial interests

315 The authors declare no competing financial interests.
316

317 ### References

318 1. Valdes AM, Walter J, Segal E, Spector TD. 2018. Role of the gut microbiota in nutrition
319 and health. BMJ 361:k2179.
320 2. Gentile CL, Weir TL. 2018. The gut microbiota at the intersection of diet and human health.
321 Science 362:776-780.
322 3. Singh RK, Chang HW, Yan D, Lee KM, Ucmak D, Wong K, Abrouk M, Farahnik B,
323 Nakamura M, Zhu TH, Bhutani T, Liao W. 2017. Influence of diet on the gut microbiome
324 and implications for human health. J Transl Med 15:73.
325 4. Spanogiannopoulos P, Bess EN, Carmody RN, Turnbaugh PJ. 2016. The microbial
326 pharmacists within us: a metagenomic view of xenobiotic metabolism. Nat Rev Microbiol
327 14:273-287.
328 5. Koppel N, Maini Rekdal V, Balskus EP. 2017. Chemical transformation of xenobiotics by
329 the human gut microbiota. Science 356.
330 6. Lam KN, Alexander M, Turnbaugh PJ. 2019. Precision Medicine Goes Microscopic:
331 Engineering the Microbiome to Improve Drug Outcomes. Cell Host Microbe 26:22-34.
332 7. Round JL, Mazmanian SK. 2009. The gut microbiota shapes intestinal immune responses
333 during health and disease. Nat Rev Immunol 9:313-323.
334 8. Hooper LV, Littman DR, Macpherson AJ. 2012. Interactions between the microbiota and
335 the immune system. Science 336:1268-1273.
336 9. Belkaid Y, Hand TW. 2014. Role of the microbiota in immunity and inflammation. Cell
337 157:121-141.
338 10. Donia MS, Fischbach MA. 2015. HUMAN MICROBIOTA. Small molecules from the
339 human microbiota. Science 349:1254766.
340 11. Garg N, Luzzatto-Knaan T, Melnik AV, Caraballo-Rodriguez AM, Floros DJ, Petras D,
341 Gregor R, Dorrestein PC, Phelan VV. 2017. Natural products as mediators of disease. Nat
342 Prod Rep 34:194-219.
343 12. Wilson MR, Zha L, Balskus EP. 2017. Natural product discovery from the human
344 microbiome. J Biol Chem 292:8546-8552.

345 13. Donia MS, Cimermancic P, Schulze CJ, Wieland Brown LC, Martin J, Mitreva M, Clardy
346 J, Linington RG, Fischbach MA. 2014. A systematic analysis of biosynthetic gene clusters
347 in the human microbiome reveals a common family of antibiotics. Cell 158:1402-1414.
348 14. Aas JA, Paster BJ, Stokes LN, Olsen I, Dewhirst FE. 2005. Defining the normal bacterial
349 flora of the oral cavity. J Clin Microbiol 43:5721-5732.
350 15. Listl S, Galloway J, Mossey PA, Marcenes W. 2015. Global economic impact of dental
351 diseases. J Dent Res 94:1355-1361.
352 16. Pitts NB, Zero DT, Marsh PD, Ekstrand K, Weintraub JA, Ramos-Gomez F, Tagami J,
353 Twetman S, Tsakos G, Ismail A. 2017. Dental caries. Nat Rev Dis Primers 3:17030.
354 17. Disease GBD, Injury I, Prevalence C. 2018. Global, regional, and national incidence,
355 prevalence, and years lived with disability for 354 diseases and injuries for 195 countries
356 and territories, 1990-2017: a systematic analysis for the Global Burden of Disease Study
357 2017. Lancet 392:1789-1858.
358 18. Bowen WH, Burne RA, Wu H, Koo H. 2018. Oral biofilms: pathogens, matrix, and
359 polymicrobial interactions in microenvironments. Trends Microbiol 26:229-242.
360 19. Banas JA, Drake DR. 2018. Are the mutans streptococci still considered relevant to
361 understanding the microbial etiology of dental caries? BMC Oral Health 18:129.
362 20. Liu L, Hao T, Xie Z, Horsman GP, Chen Y. 2016. Genome mining unveils widespread
363 natural product biosynthetic capacity in human oral microbe Streptococcus mutans. Sci
364 Rep 6:37479.
365 21. Merritt J, Qi F. 2012. The mutacins of *Streptococcus mutans*: regulation and ecology. Mol
366 Oral Microbiol 27:57-69.
367 22. Joyner PM, Liu J, Zhang Z, Merritt J, Qi F, Cichewicz RH. 2010. Mutanobactin A from
368 the human oral pathogen Streptococcus mutans is a cross-kingdom regulator of the yeast-
369 mycelium transition. Org Biomol Chem 8:5486-5489.
370 23. Hao T, Xie Z, Wang M, Liu L, Zhang Y, Wang W, Zhang Z, Zhao X, Li P, Guo Z, Gao S,
371 Lou C, Zhang G, Merritt J, Horsman GP, Chen Y. 2019. An anaerobic bacterium host
372 system for heterologous expression of natural product biosynthetic gene clusters. Nat
373 Commun 10:3665.
374 24. Lin XB, Lohans CT, Duar R, Zheng J, Vederas JC, Walter J, Ganzle M. 2015. Genetic
375 determinants of reutericyclin biosynthesis in *Lactobacillus reuteri*. Appl Environ
376 Microbiol 81:2032-2041.
377 25. Holtzel A, Ganzle MG, Nicholson GJ, Hammes WP, Jung G. 2000. The first low molecular
378 weight antibiotic from lactic acid bacteria: reutericyclin, a new tetramic acid. Angew Chem
379 Int Ed Engl 39:2766-2768.
380 26. Ganzle MG. 2004. Reutericyclin: biological activity, mode of action, and potential
381 applications. Appl Microbiol Biotechnol 64:326-332.
382 27. Argimon S, Konganti K, Chen H, Alekseyenko AV, Brown S, Caufield PW. 2014.
383 Comparative genomics of oral isolates of Streptococcus mutans by in silico genome
384 subtraction does not reveal accessory DNA associated with severe early childhood caries.
385 Infect Genet Evol 21:269-278.
386 28. Gaudelli NM, Townsend CA. 2014. Epimerization and substrate gating by a TE domain in
387 beta-lactam antibiotic biosynthesis. Nat Chem Biol 10:251-258.
388 29. Hayashi A, Saitou H, Mori T, Matano I, Sugisaki H, Maruyama K. 2012. Molecular and
389 catalytic properties of monoacetylphloroglucinol acetyltransferase from *Pseudomonas sp*.
390 YGJ3. Biosci Biotechnol Biochem 76:559-566.

30. Pavkov-Keller T, Schmidt NG, Zadlo-Dobrowolska A, Kroutil W, Gruber K. 2019. Structure and catalytic mechanism of a bacterial friedel-crafts acylase. Chembiochem 20:88-95.
31. Vilchez R, Lemme A, Ballhausen B, Thiel V, Schulz S, Jansen R, Sztajer H, Wagner-Dobler I. 2010. *Streptococcus mutans* inhibits *Candida albicans* hyphal formation by the fatty acid signaling molecule trans-2-decenoic acid (SDSF). Chembiochem 11:1552-62.
32. Zhu B, Macleod LC, Kitten T, Xu P. 2018. *Streptococcus sanguinis* biofilm formation & interaction with oral pathogens. Future Microbiol 13:915-932.
33. Lamont RJ, Koo H, Hajishengallis G. 2018. The oral microbiota: dynamic communities and host interactions. Nat Rev Microbiol 16:745-759.
34. Kreth J, Giacaman RA, Raghavan R, Merritt J. 2017. The road less traveled - defining molecular commensalism with *Streptococcus sanguinis*. Mol Oral Microbiol 32:181-196.
35. Zipperer A, Konnerth MC, Laux C, Berscheid A, Janek D, Weidenmaier C, Burian M, Schilling NA, Slavetinsky C, Marschal M, Willmann M, Kalbacher H, Schittek B, Brotz-Oesterhelt H, Grond S, Peschel A, Krismer B. 2016. Human commensals producing a novel antibiotic impair pathogen colonization. Nature 535:511-516.
36. Aleti G, Baker JL, Tang X, Alvarez R, Dinis M, Tran NC, Melnik AV, Zhong C, Ernst M, Dorrestein PC, Edlund A. 2019. Identification of the bacterial biosynthetic gene clusters of the oral microbiome illuminates the unexplored social language of bacteria during health and disease. MBio 10:e00321-19.
37. Li Y, Li Z, Yamanaka K, Xu Y, Zhang W, Vlamakis H, Kolter R, Moore BS, Qian PY. 2015. Directed natural product biosynthesis gene cluster capture and expression in the model bacterium *Bacillus subtilis*. Sci Rep 5:9383.
38. Perry D, Kuramitsu HK. 1981. Genetic transformation of *Streptococcus mutans*. Infect Immun 32:1295-1297.
39. Pfeifer BA, Admiraal SJ, Gramajo H, Cane DE, Khosla C. 2001. Biosynthesis of complex polyketides in a metabolically engineered strain of *E. coli*. Science 291:1790-2.
40. Kreth J, Zhang Y, Herzberg MC. 2008. *Streptococcal antagonism* in oral biofilms: *Streptococcus sanguinis* and *Streptococcus gordonii* interference with *Streptococcus mutans*. J Bacteriol 190:4632-40.

429 **Figure legends**

430 **Figure 1 | Identification of an orphan gene cluster from *S. mutans* and its metabolites**. (**a**)
431 Mutanocyclin gene cluster (*muc*) annotation. (**b**) HPLC profile of extracts from wild type (WT) *S.*
432 *mutans* B04Sm5 (i), *S. mutans* B04Sm5/Δ*mucD* (ii), and *S. mutans* B04Sm5/Δ*mucF* (iii). (**c**)
433 Structures of metabolites identified from *S. mutans* in this study, including reutericyclin A (**1**),
434 reutericyclin B (**2**), reutericyclin C (**3**), and mutanocyclin (**4**). C, condensation; A, adenylation; T,
435 thiolation; KS, ketosynthase; TE, thioesterase.

436

437 **Figure 2 | Model for 1-4 biosynthesis and characterization of MucF as deacetylase.** (**a**)
438 Model for the biosynthesis of **1**-**4**. (**b**) HPLC profiles of extracts from *E. coli* BAP1/pEXT06 (*mucA-*
439 *D*) (i) and *E. coli* BAP1/pEXT07 (*mucA-D+mucF*) (ii). (**c**) HPLC analysis of (i) isolated **4** as a
440 standard, (ii) compound **1** incubated with *E. coli* Rosetta2^{TM} (DE3)pLys/pET28a (empty vector)
441 cell lysate for 60 min, compound **1** incubated with *E. coli* Rosetta2^{TM} (DE3)pLys/pEXT26 (carrying
442 *mucF*) for 10 min (i), 30 min (ii), and 60 min (iii).

443

444 **Figure 3 | Interspecies competition assay.** Overnight cultures of oral commensal bacteria: *R.*
445 *mucilaginosa, S. gordonii*, and *S. sanguinis, S. mitis, S. pneumoniae,* and *S. salivarius* were
446 plated next to the indicated *S. mutans* strain (UA159, B04Sm5, Δ*mucD,* Δ*mucF*)).

447

448

449

450

451

452

453

454

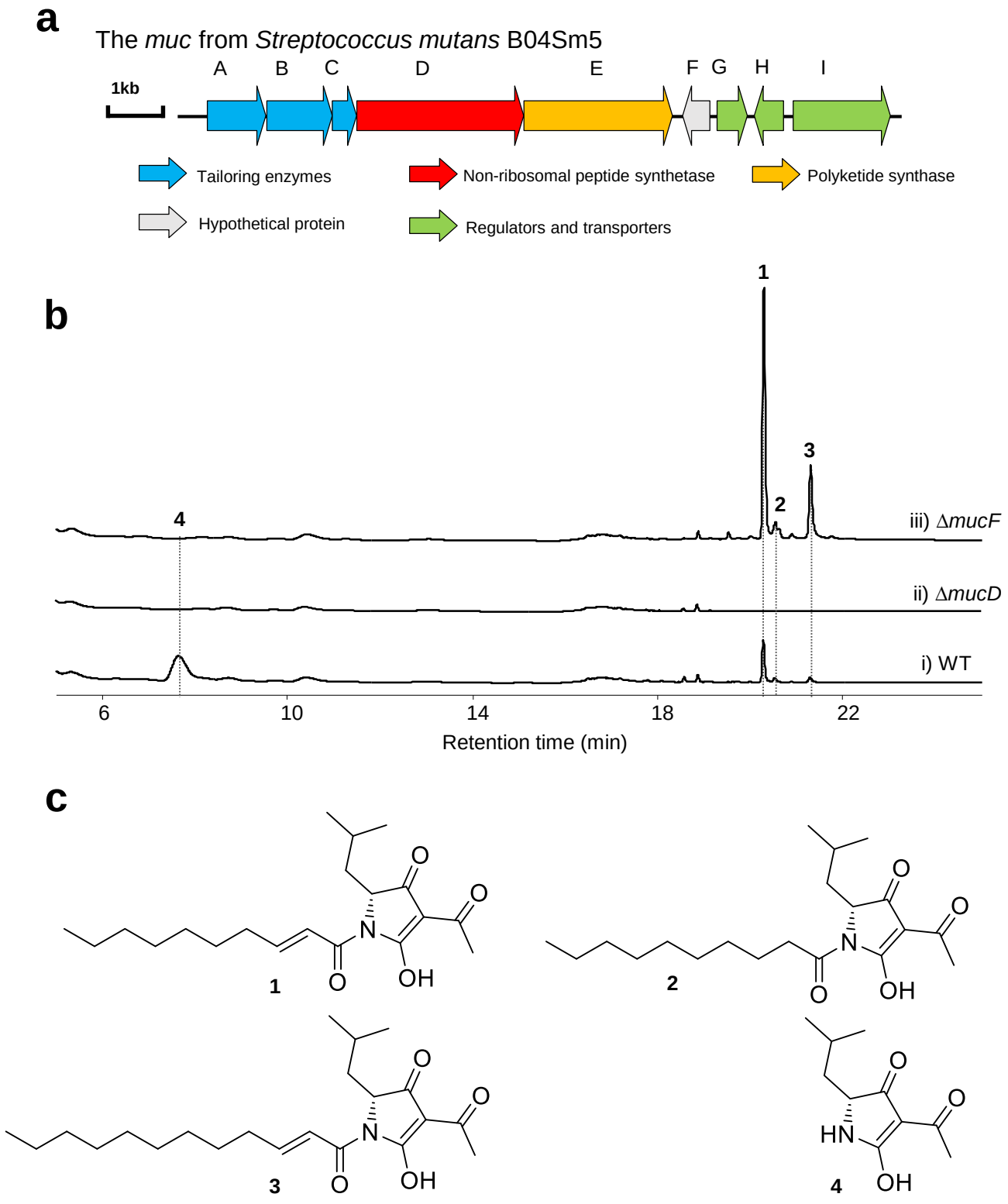
a
The muc from Streptococcus mutans B04Sm5
A
B
C
D
E
F
G
H
I
1kb
Tailoring enzymes
Non-ribosomal peptide synthetase
Polyketide synthase
Hypothetical protein
Regulators and transporters
b
1
2
3
4
iii) ΔmucF
ii) ΔmucD
i) WT
6
10
14
18
22
Retention time (min)
c
1
2
3
4
O
N
OH
HN

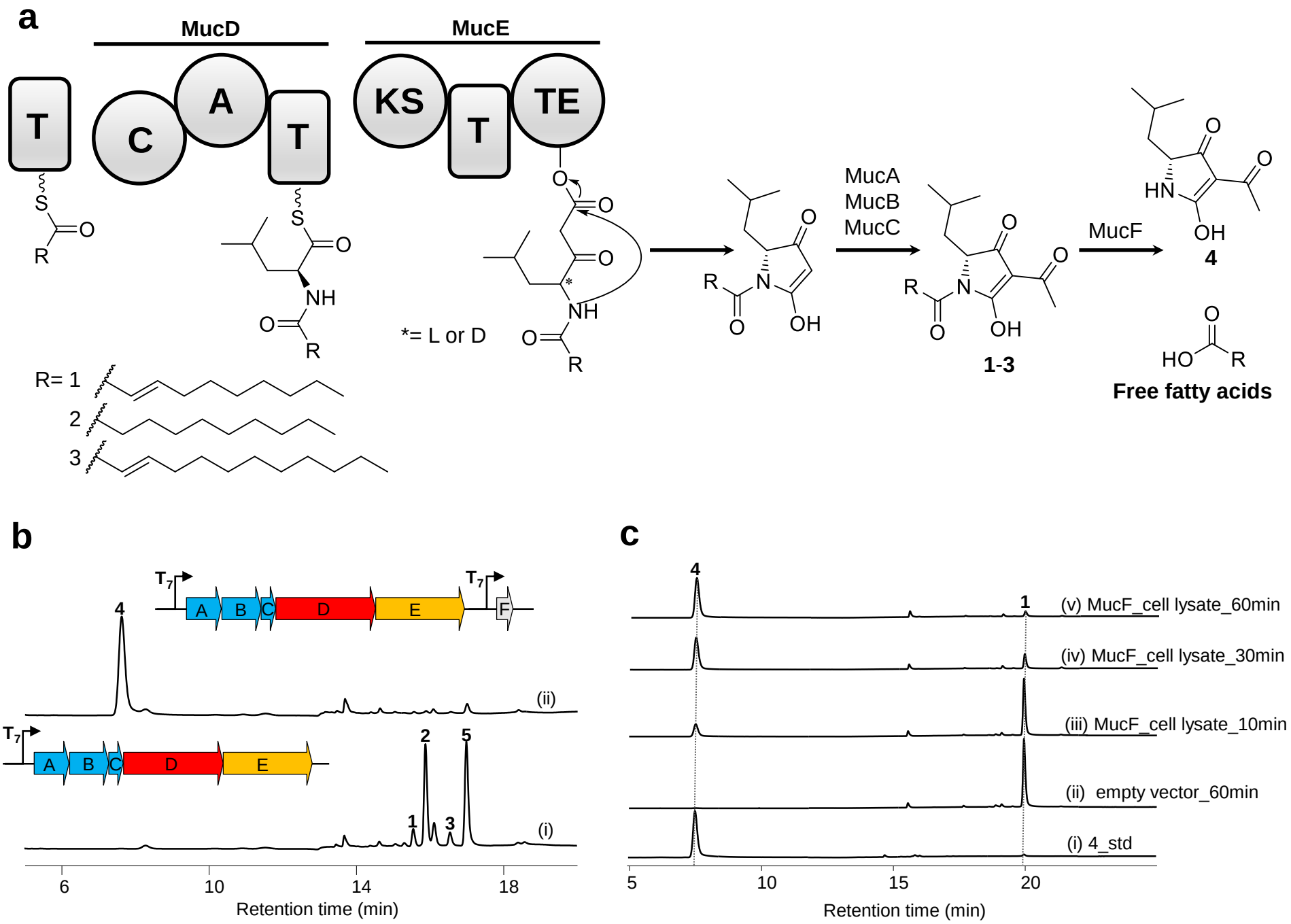
a
MucD
MucE
T
C
A
T
KS
T
TE
*= L or D
R= 1
2
3
MucA
MucB
MucC
1-3
MucF
4
Free fatty acids
b
T7
A
B
C
D
E
F
4
(ii)
2
5
1
3
(i)
6
10
14
18
Retention time (min)
c
4
1
(v) MucF_cell lysate_60min
(iv) MucF_cell lysate_30min
(iii) MucF_cell lysate_10min
(ii) empty vector_60min
(i) 4_std
5
10
15
20
Retention time (min)

R.m. = *Rothia mucilaginosa*

S.sang. = *Streptococcus sanguinis*

S.g. = *Streptococcus gordonii*

S.mit. = *Streptococcus mitis*

S.p. = *Streptococcus pneumoniae*

S.sal. = *Streptococcus salivarius*

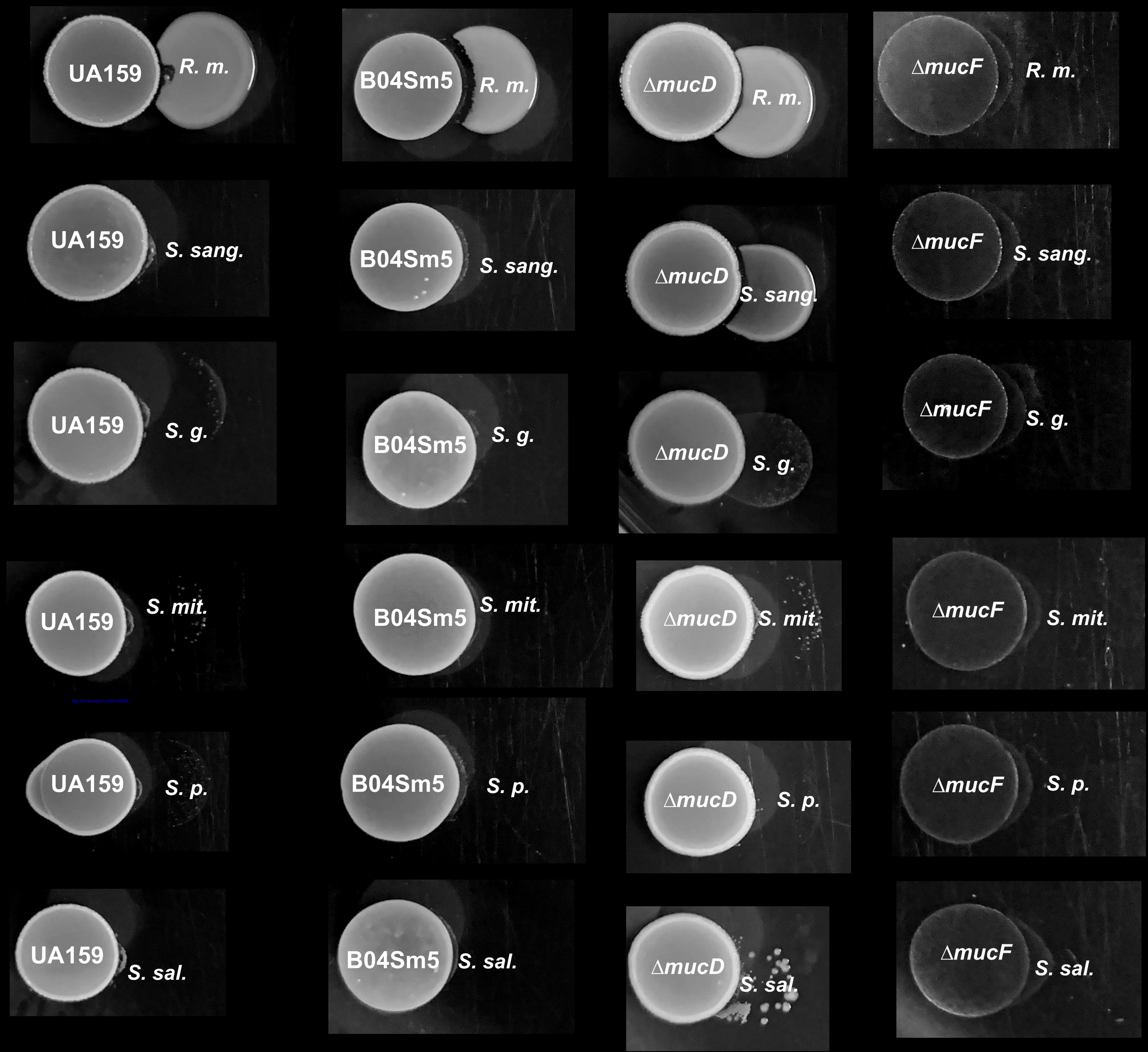

http://dx.doi.org/10.1101/755025